Impact Of Vsc-based Multiline Generalized Facts Controllers On Distance Protections

Shaik.Abbas Ali[#1],T.Ranjani[*2]

shaik.ali768@gmail.com[#1], ranjani.turumella@gmail.com[*2]

[1]Student M.tech EEE,Sree Chaitanya College Of Engineering,Karimnagar,A.P

[2]Associate Proffessor,Sree Chaitanya College Of Engineering,Karimnagr,A.P

***Abstract*—By utilizing multiline voltage-source (VSC)-based flexible ac transmission system (FACTS) controllers, independent controllability over each compensated line of a multiline system can be achieved. While VSC-based multiline FACTS controllers emerged as a new opportunity to control two independent ac systems, the main constraints and limitations that are presented to the conventional transmission-line protection systems need to be investigated. In this paper, the impacts of VSC-based FACTS controllers on distance relays while controlling the power flow of compensated lines are evaluated analytically and by detailed simulations for different fault types and locations.**

***Index Terms*—Distance relay, flexible ac transmission systems (FACTS) controllers, generalized interline power-flow controller (GIPFC), generalized unified power-flow controller (GUPFC), static compensator (STATCOM), static synchronous series compensator (SSSC).**

I. Introduction

NEW TYPES of flexible ac transmission system (FACTS) controllers have been investigated in recent years to increase power system operation flexibility and controllability, to enhance system stability, and to achieve better utilization of existing power systems [1]–[7]. However, the employment of series/shunt compensation of transmission lines by these devices creates certain problems for their protective relays and fault locators using conventional techniques because of the rapid changes introduced by the associated control actions in primary system parameters, such as line impedances and load currents. The most important singularity lays in the fact that the positive-sequence impedance measured by traditional distance relays is no longer an indicator of the distance to a fault. The apparent impedance seen by the relay is affected due to the uncertain variation of series compensation voltage during the fault period [8]–[17].

A unified power-flow controller (UPFC), which consists of a series and a shunt converter connected by a common dc-link capacitor, can simultaneously perform the function of transmission-line real/reactive power-flow control in addition to the UPFC bus voltage/shunt reactive power control. However, if power flows in more than one line need to be controlled simultaneously, UPFC seems out of its merits. Hence, multiline voltage-source (VSC)-based FACTS controllers, such as an interline power-flow controller (IPFC) [5]; generalized interline power-flow controller (GIPFC) [6], [7]; and generalized unified power-flow controller (GUPFC) [4] are introduced to control the power flows of multilines simultaneously. Multiline VSC-based FACTS controllers can control different variables of the power system, such as the bus voltage and independent active and reactive power flows of two lines by combining three or more converters working together. So it extends the concepts of voltage and power-flow control beyond what is achievable with the known two-converter UPFC controller.

Some research has been conducted to evaluate the performance of a distance relay for transmission systems with FACTS controllers. In [8], an apparent impedance calculation procedure for a transmission line with UPFC based on the power frequency sequence component is investigated; the studies include the influence of setting UPFC control parameters and the operational mode of UPFC. The work in [9] presents the operation of impedance-based protection relays in a power system containing a STATCOM; it is based on the steady-state analysis of the STATCOM and the protection relays. The work in [16] also presents steady-state analysis of the transmission-line protection in the presence of series-connected FACTS devices. In [10], the performance of distance relays of the lines compensated by two types of shunt FACTS devices, SVC and STATCOM, are investigated. In [11], the impact of FACTS devices on the tripping boundaries of distance relay is presented. The works in [12] and [13] present a comprehensive analysis of the impact of thyristor-controlled series capacitor (TCSC) on the protection of transmission lines and show that not only does the TCSC affect the protection of its line, but the protection of adjacent lines would experience problems. The studies in [14] indicate that the parameters of FACTS controllers and their location in the line (middle or line ends) have an impact on the trip boundary of a distance relay.

Fig. 1 shows the generic representation of a multiline VSC-based FACTS controller. Different controllers are achieved by the status of the dc switches, as Table I. According to this table, when all of the dc switches are closed, it represents a GUPFC [7]. SSSC1 and SSSC2 in Table I indicate the static synchronous series compensators (SSSCs) configured in *Line 1* and *Line 2*, respectively.

If *Line 1* and *Line 2* are connected to separate buses in Fig. 1, then a GIPFC is established. In the GIPFC configuration, it is possible to control the power flows of independent lines or even lines that are physically close but operate at different voltage levels.

$R1$ and $R2$ in Fig. 1 present a distance protective relay for *Line 1* and *Line 2*, respectively. In this paper, the behaviors of $R1$

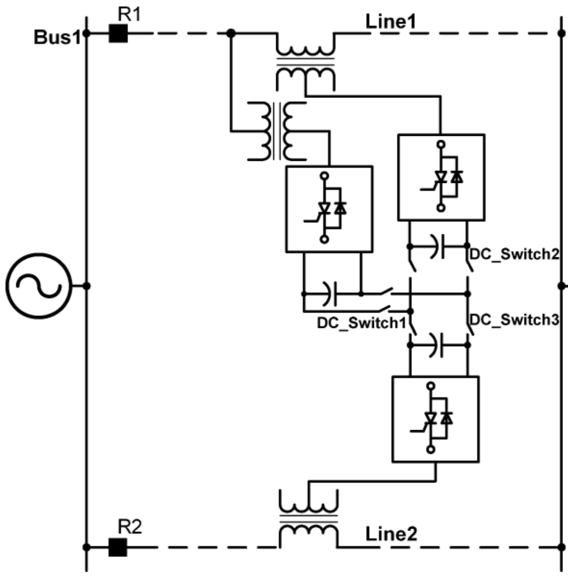

Fig. 1. Simplified one-line diagram of multiline FACTS controllers connected to the middle of the transmission lines.

TABLE I
FACTS CONTROLLERS ACHIEVED BY DIFFERENT CLOSE/OPEN CONFIGURATIONS OF DC SWITCHES IN FIG. 1

Case No.	Status of DC_Switches			FACTS Controllers
	DC_ Switch1	DC_ Switch2	DC_ Switch3	
1	Close	Close	Close	GUPFC
2	Open	Close	Close	STATCOM+IPFC
3	Close	Open	Close	UPFC extended on two lines
4	Close	Close	Open	UPFC+SSSC2
5	Open	Open	Open	STATCOM+SSSC1+SSSC2

and $R2$ during a fault on the transmission lines are investigated for different FACTS controllers according to Table I. It is worth noting that the impact of GIPFC on the protection of *Line 1* and *Line 2* could be regarded as the impact of an UPFC on relay $R1$ and an SSSC on relay $R2$, due to the fact that the *Line 1* and *Line 2* are separated from each other and not parallel. Meanwhile, the impact of GUPFC on the protective relays is more pronounced than GIPFC, because the current circulates in a loop comprising of *Line 1* and *Line 2* during different faults.

The objective of this paper is to analyze and investigate the impact of different multiline VSC-based FACTS controllers on the performance of impedance-based protection relays under normal operation and fault conditions at different load power flows. Different configurations of multiline VSC-based FACTS controllers are considered based on the cases 1 to 5 as in Table I. The controllers are modeled with detailed and sophisticated transient characteristics; the power system is designed with traveling-wave transmission-line models and advanced models are used for protective relays [18].

This paper is organized as follows. Section II explains the impact of multiline VSC-based FACTS controllers on the apparent impedance seen by the protective relays. The analysis is comprehensive and considers different effects including the mutual impedance between the lines. Section III presents sophisticated transient modeling of the series/shunt converters used

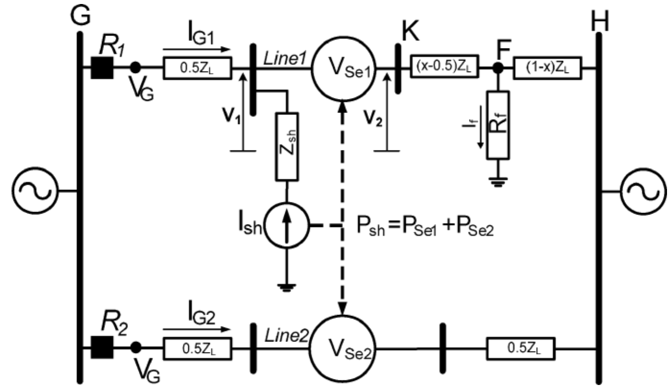

Fig. 2. Sample system with GUPFC.

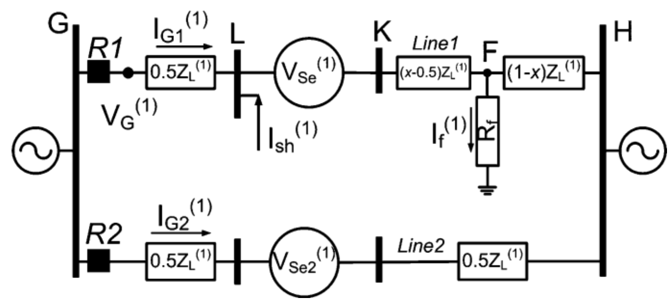

Fig. 3. Positive-sequence network of the sample system for a fault on Line1.

in the simulations. Section IV introduces the sample network. Simulation results of the sample network for different FACTS controllers based on Table I are presented in Section V.

II. MULTILINE VSC-BASED FACTS CONTROLLERS IMPACT ON APPARENT IMPEDANCE

The single-line diagram of the sample system used for the analysis is shown in Fig. 2. It consists of two parallel lines and resembles the GUPFC configuration. In this figure, the GUPFC is connected to the middle of the line to include the series compensators in the fault loop. $V_{\rm Se1}$ and $V_{\rm Se2}$ are the series-injected voltages powered by the shunt converter, represented by impedance $Z_{\rm sh}$ and current source $I_{\rm sh}$. If the converter losses are ignored, then the active power drawn by the shunt leg is equal to the delivered power to lines 1 and 2.

The performance of relays $R1$ and $R2$ for different fault types, fault locations, and fault resistances R_f is analyzed to show the impact of different multiline VSC-based FACTS controllers on distance protection. Faults on *Line 1* at point F between K and H with the per-unit distance x from the relay location are considered. In this sense, x has a value between 0.5 and 1.0 for faults between K and H in the sample system. In Fig. 2, Z_L is the impedance of each line, and V_G is the voltage measured by $R1$ and $R2$ which is the same for both relays. The positive-sequence network of the sample system of Fig. 2 is shown in Fig. 3.

The negative-sequence network is the same as Fig. 3, except that the superscripts are changed to 2. The zero-sequence network of the sample system of Fig. 2 is shown in Fig. 4. $Z_m^{(0)}$

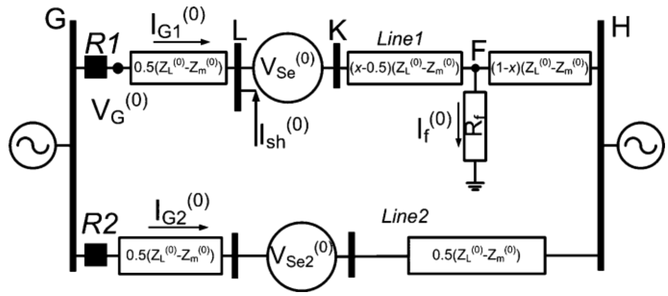

Fig. 4. Zero-sequence network of the sample system.

is the zero-sequence mutual impedance between the ground wire(s) and the faulted phase conductor, per span of the lines.

The positive-sequence voltage at the relay point $R1$ can be expressed as follows:

$$V_G^{(1)} = I_{G1}^{(1)}\left(0.5Z_L^{(1)}\right) + \left(I_{G1}^{(1)} + I_{sh}^{(1)}\right) \times \left((x-0.5)\, Z_L^{(1)}\right) + V_G^{(1)} + R_f I_f^{(1)}. \quad (1)$$

The positive-sequence mutual impedance of the lines $Z_m^{(1)}$ is negligible with respect to $Z_m^{(1)}$, so it is ignored in (1). Negative-sequence voltage $V_G^{(1)}$ is the same as (1), except that the superscripts are changed to 2. Zero-sequence voltage $V_G^{(1)}$ is as follows:

$$V_G^{(1)} = I_{G1}^{(1)}\left(0.5\left(Z_L^{(0)} - Z_m^{(0)}\right)\right) + \left(I_{G1}^{(1)} + I_{sh}^{(1)}\right) \times \left((x-0.5)\left(Z_L^{(0)} - Z_m^{(0)}\right)\right) + V_G^{(1)} + R_f I_f^{(1)}. \quad (2)$$

For a single-phase fault, the following equations can be used:

$$V_G^{(1)} + V_G^{(1)} + V_G^{(0)} = V_G \quad (3)$$

$$I_{G1}^{(1)} + I_{G1}^{(1)} + I_{G1}^{(0)} = I_{G1}. \quad (4)$$

Using the previous equations, we have

$$V_G = I_{G1}\left(xZ_L^{(1)}\right) + I_{G1}^{(1)}\left[x\left(Z_L^{(0)} - Z_L^{(0)} - Z_m^{(0)}\right)\right] + I_{sh}(x-0.5)\, Z_L^{(0)} + I_{sh}^{(0)}\left[(x-0.5)\left(Z_L^{(0)} - Z_L^{(0)} - Z_m^{(0)}\right)\right] + V_{Se1} + R_f I_f. \quad (5)$$

A. Single-Phase Fault

For a single-phase fault on *line 1*, the apparent impedance seen by relay $R1$ is as follows:

$$Z_{R1} = \frac{V_G}{I_{G1} + \left(\frac{Z_L^{(0)} - Z_L^{(1)}}{Z_L^{(1)}}\right) I_{G1}^{(1)}} = \frac{V_G}{I_{R1}}. \quad (6)$$

Using (5) in (6), we have

$$Z_{R1} = xZ_L^{(0)} - xZ_m^{(0)}\frac{I_{G1}^{(1)}}{I_{R1}} + \frac{I_{sh}}{I_{R1}}(x-0.5)Z_L^{(0)} + \frac{I_{G1}^{(1)}}{I_{R1}}(x-0.5)\left(Z_L^{(0)} - Z_L^{(0)} - Z_m^{(0)}\right) + \frac{V_{Se1}}{I_{R1}} + R_f\frac{I_f}{I_{R1}}. \quad (7)$$

From (7), we see that the apparent impedance seen by the traditional distance relay $R1$ during a single-phase fault when applied to the transmission system employing GUPFC as one of the multiline VSC-based FACTS controllers, has six components:

1) $xZ_L^{(0)}$: Positive-sequence impedance from the relay point to the fault point, which should be the correct value for the distance relay;
2) $xZ_m^{(0)}(I_{G1}^{(0)})/(I_{R1})$: This part is the impact of zero-sequence mutual impedance of the transmission lines, which can be treated the same as the uncompensated lines;
3) $(I_{sh})(x-0.5)Z_L^{(1)}/(I_{R1})$: The shunt current I_{sh} injected by the shunt converter of the GUPFC, which has a direct impact on the apparent impedance.
4) $(I_{sh}^{(0)})(x-0.5)(Z_L^{(0)} - Z_L^{(0)} - Z_m^{(0)})/(I_{R1})$: This part relates to the impact of zero-sequence current injected by the shunt converter of the GUPFC; in practice, one side of the shunt transformer of the GUPFC often has a delta connection, so there is no zero-sequence current injected by this shunt leg, and this part can be neglected;
5) $(V_{Se1})/(I_{R1})$: The injected series voltage of the GUPFC has a direct impact on the apparent impedance;
6) $R_f(I_f)/(I_{R1})$: The last part of the apparent impedance is caused by fault resistance.

For a single-phase fault on *Line 2*, the analysis will be the same. The apparent impedance seen by $R2$ for a single-phase fault is represented by

$$Z_{R2} = xZ_L^{(0)} + xZ_m^{(0)}\frac{I_{G1}^{(1)}}{I_{R2}} + \frac{V_{Se2}}{I_{R2}} + R_f\frac{I_f}{I_{R2}}. \quad (8)$$

It means that the impact of GUPFC on relay $R2$ is only due to the injected series voltage of GUPFC and the contribution of GUPFC to the fault current. In other words, the impact of injected shunt current I_{sh} on Z_{R2} is negligible for solid faults. However, I_{sh} directly affects Z_{R1} even if $R_f = 0$. This is a major difference between (7) and (8). It can also be seen from (8) that the series-injected voltage V_{Se2} is directly added to the apparent impedance $Z_L^{(0)}$; hence increasing the apparent impedance seen by the relay.

If the GUPFC in the sample system is replaced by an IPFC, then the injected shunt current I_{sh} will be zero and the effect of the IPFC on the apparent impedance is only through the series-injected voltages V_{Se1} or V_{Se2}.

B. Phase-to-Phase Fault

The apparent impedance seen by $R1$ for a phase-to-phase fault, such as A-B, is expressed as

$$Z_{R1(A-B)} = \frac{V_A - V_B}{I_A - I_B} = \frac{V_{relay}}{I_{relay}} = \frac{V_G^{(1)} - aV_G^{(2)}}{I_{G1}^{(1)} - aI_{G1}^{(2)}} \quad (9)$$

where $a = 1\angle 120° = -0.5 + j0.886. V_A, V_B, I_A$ and I_B are the voltages and currents of phases A and B at the relay point, respectively. Using (1), we have

$$V_G^{(1)} - aV_G^{(2)} = xZ_{L1}^{(1)}\left(I_{G1}^{(1)} - aI_{G1}^{(2)}\right) + \left(I_{Sh}^{(1)} - aI_{Sh}^{(2)}\right)\dots (x-0.5)Z_{L1}^{(1)} + \left(V_{Se1}^{(1)} - aV_{Se2}^{(2)}\right) + \left(I_f^{(1)} - aI_f^{(2)}\right)R_f. \quad (10)$$

R_f is the fault resistance between two phases in (10). Hence, the apparent impedance for a phase-to-phase (A-B) fault is

$$Z_{R1(A-B)} = xZ^{(1)}_{L1} + \frac{\left(I^{(1)}_{\text{Sh}} - aI^{(2)}_{\text{Sh}}\right)}{I_{\text{relay}}}(x \quad 0.5)Z^{(1)}_{L1} + \frac{\left(V^{(1)}_{\text{Se1}} \quad aV^{(2)}_{\text{Se1}}\right)}{I_{\text{relay}}} + \frac{I^{(1)}_f \quad aI^{(2)}_f}{I_{\text{relay}}}R_f. \quad (11)$$

From (11), we can conclude that during a phase-to-phase fault, the apparent impedance seen by $R1$ is composed of four parts: the first is positive-sequence impedance from the relay point to fault point, which should be the correct value for the relay; the second part is the impact of shunt converter on the apparent impedance and depends upon the difference between the positive- and negative-sequence currents injected by the shunt leg; the third is proportional to the difference between the positive- and negative-sequence voltages injected by the series converter; and the last part of the apparent impedance is caused by the fault resistance. For a solid phase-to-phase fault, the impact of GUPFC on the apparent impedance is expressed by $(I^{(1)}_{\text{Sh}} \quad aI^{(2)}_{\text{Sh}})/(I_{\text{Relay}})$ and $(V^{(1)}_{\text{Se1}} \quad aV^{(2)}_{\text{Se1}})/(I_{\text{relay}})$, which are less significant with respect to a single-phase fault. In other words, the impact of GUPFC on the apparent impedance is more pronounced for single-phase faults than phase-to-phase faults. For $R2$, the shunt converter contribution to the apparent impedance is not available so the impact is only due to the series part $(V^{(1)}_{\text{Se1}} \quad aV^{(2)}_{\text{Se1}})/(I_{\text{relay}})$.

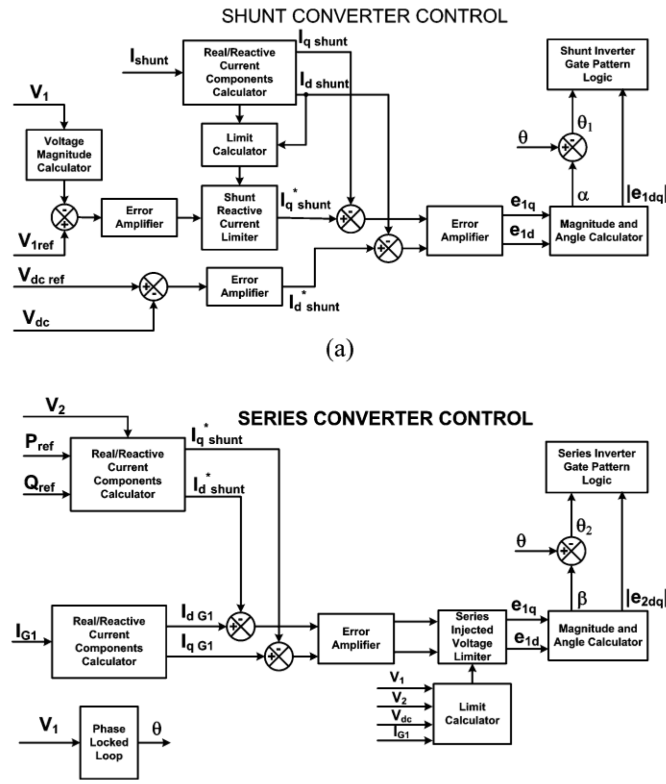

Fig. 5. Control systems used for GUPFC converters. (a) Shunt converter control system. (b) Series converter control system.

III. GUPFC Control System

Although GUPFC has many possible operating modes, it is anticipated that the shunt converter will generally operate in automatic voltage-control mode and the series converter will typically be in automatic power-flow control mode. Accordingly, block diagrams are shown in Fig. 5(a) and (b), giving greater detail of the control schemes for each converter operating in these modes. The control schemes assume that series and shunt converters generate output voltage with controllable magnitude and angle, and that the dc bus voltage will be held substantially constant [19].

The automatic power-flow control for the series converter is achieved by means of a vector-control scheme that regulates the transmission-line current, using a synchronous reference frame in which the control quantities appear as dc signals in the steady state. The appropriate real and reactive current components are determined for a desired P_{ref} and Q_{ref}, compared with the measured line currents, and used to derive the magnitude and angle of the series converter voltage. The series-injected voltage limiter in the forward path of this controller takes practical limits on series voltage into account. This is an important point in analyzing the impact of GUPFC on the performance of distance relay, ignoring the role of the "series injected voltage limiter" block in Fig. 5(b), overestimating the impact of GUPFC, and leading to unrealistic exaggerated results, creating overrated concerns for utilities.

A vector-control scheme is also used for the shunt converter. In this case, the controlled current is the current delivered to the line by the shunt converter. In this case, however, the real and reactive components of the shunt current have a different significance. The reference for the reactive current I_{qshunt} is generated by an outer voltage-control loop, responsible for regulating the ac bus voltage and the reference for the real power-bearing current I_{dshunt} is generated by a second voltage-con- trol loop that regulates the dc bus voltage. In particular, the real power negotiated by the shunt converter is regulated to balance the dc power from the series converter and maintain a desired bus voltage. The dc voltage reference $V_{\text{dc ref}}$ may be kept sub- stantially constant. For the shunt converter, the most important limit is the limit on shunt reactive current, nominated by the "shunt reactive current limiter" block in Fig. 5(a), as a func- tion of the real power being passed through the dc bus. This prevents the shunt converter current reference from exceeding its maximum rated value. The current limiter in the shunt con- trol system is used to restrict $\sqrt{I^2_{\text{dshunt}} + I^2_{\text{qshunt}}}$ in a specified value. In normal operating conditions, active current (I_{dshunt}) is very small. So $\sqrt{I^2_{\text{dshunt}} + I^2_{\text{qshunt}}}$ is approximately equal to I_{qshunt}. However, when a fault occurs on the line, I_{dshunt} is increased due to the power system unbalance condition. In contrast to I_{qshunt}, I_{dshunt} is not controllable. Therefore, in order to limit $\sqrt{I^2_{\text{dshunt}} + I^2_{\text{qshunt}}}$, I_{qshunt} should be decreased.

The control block diagrams shown in Fig. 5(a) and (b) are only a small part of the numerous control algorithms that are needed for all of the operating modes of the GUPFC, and for protection and sequencing. The control system typically incorporates many sophisticated elements that comprise the dynamics of a multiline FACTS controller [19].

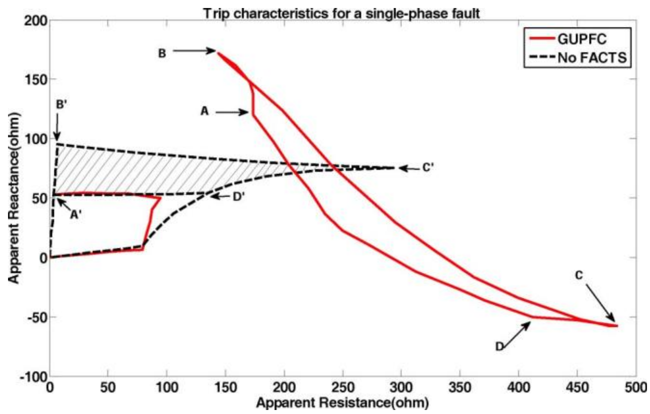

Fig. 6. Trip characteristics of relay for a single-phase fault.

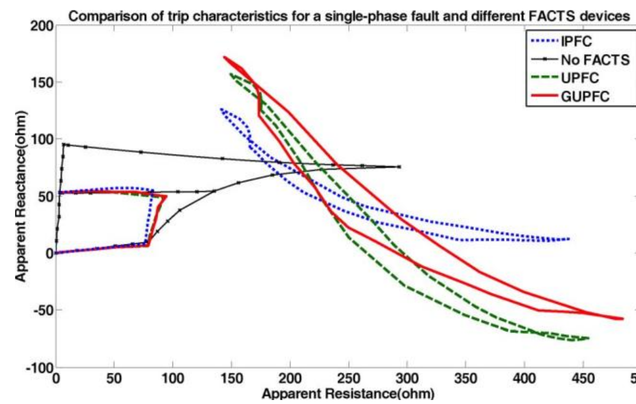

Fig. 7. Comparison of trip characteristics of relay R1 for a single-phase fault and different multiline FACTS controllers.

IV. Sample System

The sample system used for simulation is as Fig. 2. It is simulated in the *MATLAB/Simulink* environment using the *SimPowerSystems* toolbox and discrete modeling with detailed representation of the components [20]. The 300 km, 500 kV double-circuit transmission lines and the sources have the following positive- and zero-sequence impedances:

- $Z_L^{(1)} = 0.02546 + j0.352\,\Omega z/km$, $Z_L^{(0)} = 0.3864 + j1.5556\,\Omega/km$,
- $Z_G^{(1)} = 1.7431 + j19.424\,\Omega$, $Z_G^{(0)} = 2.6147 + j4.886\,\Omega$,
- $Z_H^{(1)} = 0.8716 + j9.7120\,\Omega$, $Z_H^{(0)} = 1.3074 + j2.4430\,\Omega$,
- load angle between the sources is 20°.

V. Simulation Results

The simulations are performed on the sample system of Fig. 2. In analyzing the impact of different FACTS controllers (GUPFC, UPFC and IPFC) on the performance of distance relay $R1$, the reference values of the active and reactive powers $P_{\rm ref}$ and $Q_{\rm ref}$ of the transmission lines, associated with the series converters [Fig. 5(b)] and the reference voltage value $V_{1\rm ref}$ of the shunt converter are fixed at the same values, so the power flows and the related bus voltage are the same for the normal cases. After the fault, the power flows and the controlled bus voltage change, hence the associated series/shunt controllers attempt to bring them to pre-fault values, resulting different impacts on the apparent impedance seen by the relay based on the configuration of the related FACTS controller.

A. Relay Performance for a Single-Phase Fault (A-G)

Fig. 6 shows the trip characteristics for a single-phase fault for the system with/without GUPFC. As can be seen from this figure, the GUPFC in the middle of the line caused the trip characteristics to be split into two completely separate parts. Section A-B is the trajectory for faults with R_f =0 from 150 km (middle of the line) up to 270 km (90% of the line) (e.g., point A is the apparent impedance seen by relay $R1$ for a solid single-phase fault at 150 km comprises GUPFC in the fault loop). Section B-C is for single-phase faults at 270 km for $R_f = 0$ up to 200 Ω, section C-D is for the same faults with $R_f = 200\,\Omega$ from 270 km down to 150 km and, finally, section D-A is for faults with $R_f =$ 200Ω down to $R_f =$ 0 at 150 km [21].

A comparison of the characteristics *ABCD* with its counterpart $A'B'C'D'$ (hatched area without GUPFC) reveals that GUPFC has an impact on $R1$ to measure higher apparent reactance/resistance. This means for a single-phase fault at *Zone I* reach of the relay, higher apparent impedance is seen by the relay, so the fault falsely appears outside *Zone I*. In other words, GUPFC causes the relay to underreach.

Comparing the section B-C with B'-C' shows that when the fault resistance is increased for the system without flexible ac transmission system (FACTS) controllers, the related section linearly expands from B' to C' with a nearly constant reactance, while, for the system with GUPFC, the trajectory moves forward from B to C with a sharp decline in the reactance, even leading to negative reactance values.

The trip characteristics of the sample system with UPFC and IPFC are also extracted and superimposed on Fig. 6 for comparison. Fig. 7 shows the results. It can be observed that the impact of GUPFC on the trip characteristics for a single-phase fault is the most severe, while the impact of IPFC is the least. This is due to the intervention of the shunt controller in the case of GUPFC/UPFC to keep the associated bus voltage constant, while, IPFC does not have a shunt converter, so its impact is only through the injected voltage from the series converter.

It is worth noting that the impact of the FACTS controllers on the trip characteristics of the first half of the transmission line is only through the fault resistance R_f.

B. Relay Performance for Two-Phase Faults (A-B)

Fig. 8 shows the apparent impedance seen by relay $R1$ in the sample system of Fig. 2 for a two-phase fault (A-B) at 225 km (75% of the 300 km line) from the relay with *Zone I* setting $= 0.8 * 300 = 240$ km for different FACTS controllers. It can be seen that the trajectories of apparent impedances do not enter the *Zone I* mho characteristics for GUPFC/UPFC, while the trajectory does enter the circle for IPFC. It can be deduced that

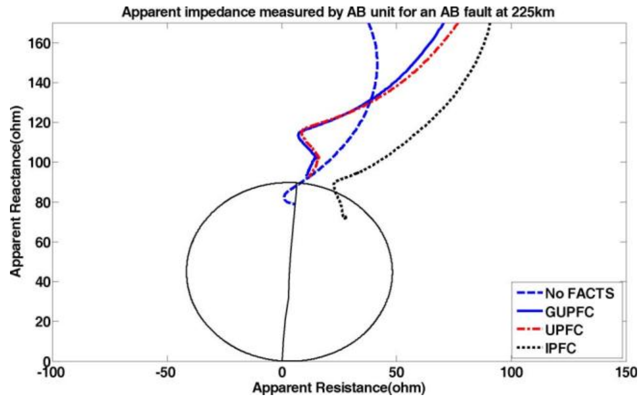

Fig. 8. Apparent impedance seen by for a phase-to-phase fault at 225 km.

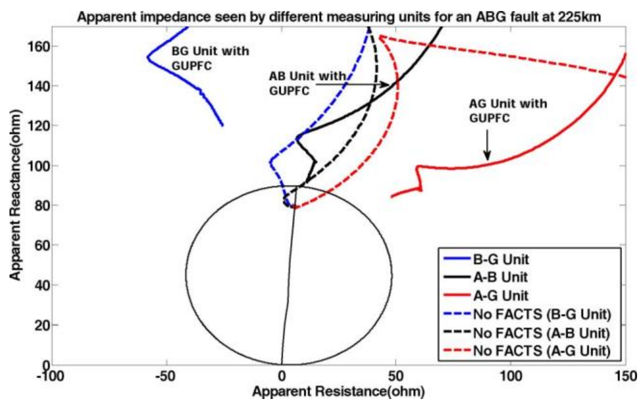

Fig. 9. Apparent impedance seen by different measuring units of the relay for an *ABG* fault at 225 km with GUPFC.

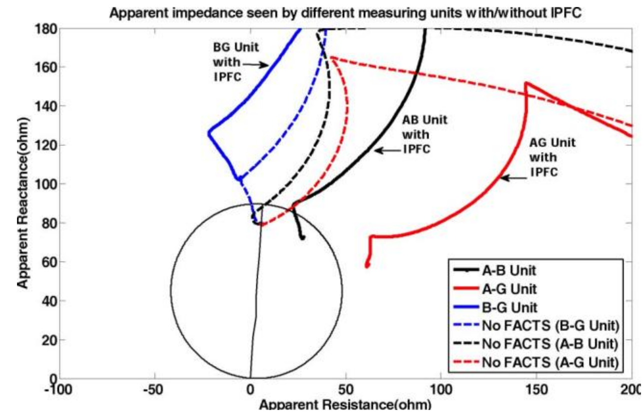

Fig. 10. Apparent impedance seen by different measuring units of the relay for an *ABG* fault at 225 km with IPFC.

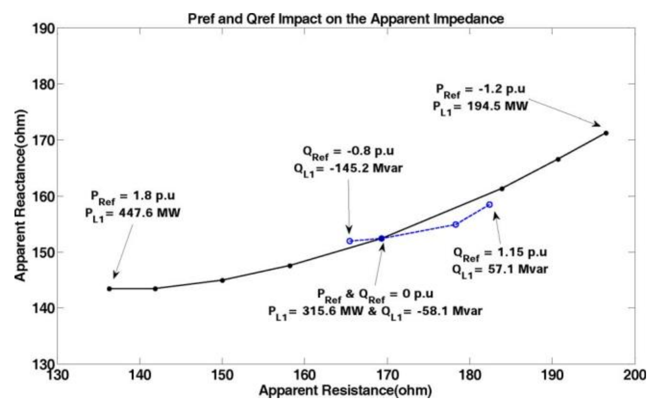

Fig. 11. Apparent impedance seen by distance relay for different values of active and reactive power-flow reference values.

GUPFC/UPFC caused the relay to underreach (i.e., not to detect the fault at *Zone I*), while the impact of IPFC is not remarkable.

C. Relay Performance for Two-Phase-to-Ground Faults

Fig. 9 shows the case for a two-phase-to-ground fault (*ABG*) at 225 km from $R1$ for different relay measuring units (i.e., A-B are responsible for monitoring phase-to-phase faults, and A-G and B-G are dedicated to single-phase faults. It is well worth reminding that the conventional full-scheme distance relays have six measuring units, that is, three for single-phase faults (A-G, B-G and C-G) and three phase-to-phase measuring units (A-B, B-C and C-A). The other fault types are detected by a combination of these six measuring units.

As can be deduced from Fig. 9, the impact of GUPFC for *ABG* faults is less severe than the single-phase faults. Despite the fact that the A-B unit does not cross the trip boundary, it is still less affected than the single-phase measuring units (A-G and B-G).

If GUPFC is replaced by IPFC (i.e., the shunt converter is put out of action), the A-B measuring unit enters the mho circle and the relay detects the fault at *Zone I* according to Fig. 10. This indicates that in the case of IPFC, the relay is less affected for two-phase-to-ground faults. This case can be justified by the fact that the IPFC does not have a shunt converter to control the bus voltage that it is attached to ($V1$ in Fig. 2), so there is less intervention from the multiline FACTS controllers on the natural behavior of the power system during faults.

D. Impact of $P_{\rm ref}$ and $Q_{\rm ref}$ on the Apparent Impedance

The apparent impedance seen by the distance relay is extracted for a single-phase fault at 225 km for different values of active power flow on *Line 1*. In order to investigate the impact of $P_{\rm ref}$ individually, $Q_{\rm ref}$ is kept constant for different values of $P_{\rm ref}$ within the permissible limits. Fig. 11 shows the simulation results. As can be seen from this figure, for $P_{\rm ref} = Q_{\rm ref} = 0$, the power flows are 315.6 MW and 58.1 MVAr. The solid line in Fig. 11 shows the variation of the apparent impedance versus the variation of $P_{\rm ref}$, while keeping $Q_{\rm ref}$ constant. It can be deduced that $P_{\rm ref}$ has an impact on the apparent impedance for all of the values between 1.8 p.u. and 1.2 p.u. with a constant $Q_{\rm ref}$. This impact is more pronounced for lower values of $P_{\rm ref}$. It is worth noting that the specified range of $+1.8$ p.u. to 1.2 p.u. is the permissible distant that GUPFC can follow $P_{\rm ref}$ with fixed $Q_{\rm ref}$. In the next step, $Q_{\rm ref}$ is varied while $P_{\rm ref}$ is held constant. The permissible range of $Q_{\rm ref}$ for a fixed value of $P_{\rm ref}$ is 0.8 p.u. to 1.15 p.u. As Fig. 11 shows, $Q_{\rm ref}$ also affects the apparent impedance such as $P_{\rm ref}$ but to a lesser extent. The impact of $Q_{\rm ref}$ is higher for its lower values.

E. Impact of Limiters of the Series and Shunt Converters on the Apparent Impedance

As mentioned in Section III, the limiters in Figs. 5(a) and (b) have an extraordinary effect on the performance evaluation of

Fig. 12. Impact of "shunt reactive current limiter" block on the measured apparent impedance.

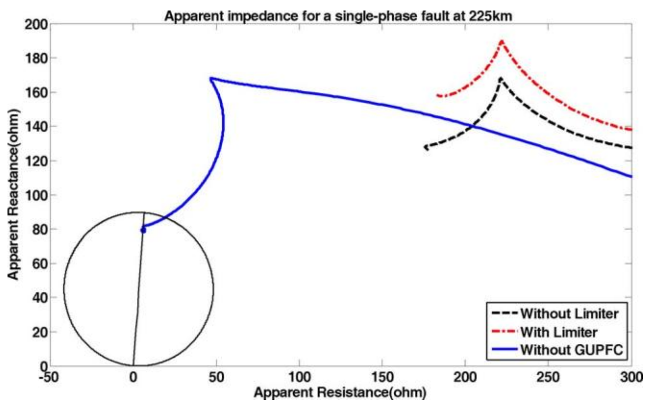

Fig. 13. Apparent impedance for an A-G fault at 225 km with and without a "shunt reactive current limiter" and "series injected voltage limiter" blocks.

the relay. The simulations are performed by bypassing them for comparison. As already mentioned, the impact of the shunt converter limiter is more pronounced. Fig. 12 shows the apparent impedance seen by $V1$ for a single-phase fault at 225 km on *Line 1* compensated by GUPFC with/without limiter on the shunt converter. As can be deduced from this figure, negligence of the "shunt reactive current limiter" block in Fig. 5(a) causes the relay measuring system to overestimate the effect of GUPFC (i.e., relay underreaches and is not able to detect the fault at *Zone I*). Meanwhile, the detailed and accurate modeling of the GUPFC dynamics and practical constraints lead to a more realistic result and demonstrate the correct operation of the relay by indicating that the apparent impedance trajectory crosses the trip boundary. As Fig. 12 shows, the omission of the shunt limiter means there is no bound on the GUPFC injecting shunt current during the fault.

Fig. 13 shows the apparent impedance for a single-phase fault at 225 km with/without implementing "shunt reactive current limiter" and "series injected voltage limiter" blocks as in Fig. 5. The overall result is that the relay underreaches when GUPFC is used for system compensation, with/without limiters. Bypassing the limiters in this case has a hybrid influence on the apparent impedance. As can be deduced from Fig. 13, there is no remarkable difference between the system with series and shunt limiters and the system without both of them. This means the deficiency of neglecting the shunt limiter is compensated by omitting the series limiter, henceforth, the overall effect is not so appreciable

VI. Conclusion

In this paper, it is shown that multiline VSC- based FACTS controllers, which are used to simultaneously control the active and reactive power flows of multilines, have a remarkable impact on conventional distance protection of transmission lines due to the rapid changes introduced by the associated control actions in primary system parameters such as line impedances and load currents. GUPFC, IPFC, and UPFC are analyzed as samples of multiline FACTS controllers. The following points are concluded from this study.

- GUPFCm, when installed in the middle of the line, causes the trip characteristics to be split into two completely separate parts.
- The GUPFC impact on the apparent impedance measured by the relay is higher reactance/resistance. In other words, GUPFC causes the relay to underreach.
- The impact of the active power reference value $P_{\mathbf{ref}}$ on the measured apparent impedance is more pronounced for lower values than the high values.
- GUPFC impact on the apparent impedance is mainly due to the zero-sequence component of the injected voltage during the fault which is caused by the unbalanced condition imposed by the GUPFC output voltage. This is due to the simultaneous three-phase compensation of GUPFC.
- Negligence of the "shunt reactive current limiter" block in the shunt converter control system causes the relay measuring system to overestimate the effect of GUPFC (i.e., the relay underreaches abnormally and is not able to detect the fault at *Zone I* for an overrated distance).
- Detailed and accurate modeling of the GUPFC dynamics and imposing practical constraints lead to a more realistic result and demonstrate the correct operation of the relay for faults at *Zone I*.
- In the case of IPFC, the relay is less affected for different faults, especially, two-phase-to-ground faults. This is due to the fact that the IPFC does not have a shunt converter to control the bus voltage that it is attached to, so there is less intervention from the multiline FACTS controllers on the natural behavior of the power system during faults.
- The impact of GUPFC is the most severe and the impact of IPFC is the least. This is due to the intervention of the shunt controller in the case of GUPFC/UPFC.
- The impact of the FACTS controllers on the trip characteristics of the first half of the transmission line is only through the fault resistance R_f.

References

[1] N. G. Hingorani and L. Gyugyi, *Understanding FACTS: Concepts and Technology of Flexible AC Transmission Systems*. Piscataway, NJ: IEEE Press, 2000.

[2] K. K. Sen, "SSSC—Static synchronous static compensator: Theory, modeling, and applications," *IEEE Trans. Power Del.*, vol. 13, no. 1, pp. 241–246, Jan. 1998.

[3] Static Synchronous Series Compensator (SSSC), CIGRE Brochure, Working Group B4.40 no. 371, Feb. 2009.

